Rectification properties of geometrically asymmetric metal–vacuum–metal junctions: a comparison of tungsten and silver tips to determine the effects of polarization resonances

2009 J. Phys.: Condens. Matter 21 395304

(http://iopscience.iop.org/0953-8984/21/39/395304)

IOP Publishing Journal of Physics: Condensed Matter

J. Phys.: Condens. Matter **21** (2009) 395304 (7pp) doi:10.1088/0953-8984/21/39/395304

Rectification properties of geometrically asymmetric metal–vacuum–metal junctions: a comparison of tungsten and silver tips to determine the effects of polarization resonances

A Mayer[1,3] **and P H Cutler**[2]

[1] FUNDP—University of Namur, Rue de Bruxelles 61, B-5000 Namur, Belgium
[2] 104 Davey Laboratory, The Pennsylvania State University, University Park, PA 16802, USA

E-mail: alexandre.mayer@fundp.ac.be

Received 9 June 2009, in final form 25 August 2009
Published 8 September 2009
Online at stacks.iop.org/JPhysCM/21/395304

Abstract

We simulate with a transfer-matrix methodology the rectification properties of geometrically asymmetric metal–vacuum–metal junctions in which one of the metals is flat while the other is extended by a tip. We consider both tungsten and silver as the material for the tip and we study the influence of the dielectric function of these materials on the rectification properties of the junction. We determine in particular the power that these junctions could provide to an external load when subject to a bias whose typical frequency is in the infrared or optical domain. We also study the rectification ratio of these junctions, which characterizes their ability to rectify the external bias by providing currents with a strong dc component. The results show that these quantities exhibit a significant enhancement for frequencies Ω that correspond to a resonant polarization of the tip. With silver and the geometry considered in this paper, this arises for $\hbar\Omega$ values of the order of 3.1 eV in the visible range. Our results hence indicate that the frequency at which the device is the most efficient for the rectification of external signals could be controlled by the geometry or the material used for the tip.

(Some figures in this article are in colour only in the electronic version)

1. Introduction

There is a growing demand for high-speed electronics. The need to eventually couple photonic and electronic circuits require in particular the development of devices that can respond to electromagnetic stimulations, whose typical frequencies are in the infrared or optical domain. There is in this context a renewed interest for point-contact diodes. These systems were originally designed as metal–oxide–metal systems in which one of the metals is essentially flat while the other is extended by a sharp tip [1]. Because of their geometrical asymmetry, these systems act as rectifiers when subject to an oscillating bias [2–6] and their main applications have essentially included the detection, the rectification and the frequency mixing of infrared radiation [7–12].

The rectification properties of these junctions are essentially due to the difference in the potential barrier seen by electrons traveling in the forward versus the backward directions [2–6]. A cut-off of this rectification is expected when the frequency is so high that the bias reverses before the electron has been able to transit through the device [4, 13]. Since tunneling times are typically of the order of 10^{-15} s [4, 13, 14], this cut-off may appear at frequencies as high as 10^{15} Hz if the cathode–anode spacing is sufficiently small, so that rectification up to the optical frequencies can in principle be achieved [4–6].

[3] Author to whom any correspondence should be addressed.

In previous publications [5, 6], a transfer-matrix methodology was developed that enables a detailed quantum-mechanical analysis of geometrically asymmetric metal–vacuum–metal junctions that are subject to an oscillating bias. This work confirmed that these systems act as rectifiers up to optical frequencies and we settled the basis for a more systematic exploration of this rectification. We extend this study by investigating the influence of the dielectric function of the material considered for the tip. We compare in particular the rectification achieved when tungsten or silver is used as material for the tip. Silver was considered because of the presence of plasmons [15] in the range of frequencies at which the junction is the most efficient for the rectification of external signals. This study aimed at determining the role of these plasmons and more generally of the frequency-dependence of the dielectric function on the rectification properties of the junction.

This paper is organized according to the following lines. In section 2, we present the methodology used to simulate metal–vacuum–metal junctions that are subject to an oscillating bias. The methodology is extended in order to account for the complex-valued dielectric function that describes the material used for the tip. In section 3, we consider tungsten as material for the tip and we study the influence of the dielectric function of this material on the rectification properties of the junction. In section 4, we consider silver as material for the tip. Compared to the results obtained with tungsten, the power gained by the electrons that cross the device as well as the rectification ratio of this device turn out to be enhanced by several orders of magnitude at frequencies that correspond to a resonant polarization of the tip. These results suggest that the dependence of the plasmon frequencies on both the material and the geometry of the tip could be used to control the frequency at which the junction is the most efficient for the rectification of external signals. This opens the possibility the build devices of the type presented in this paper for the selective detection of radiations in the infrared or visible domain or for a more efficient conversion of their energy.

2. Methodology

The systems we consider in this work consist of two metals that are separated by a vacuum gap of length D. We refer by $z = 0$ and D to the flat parallel surfaces of these metals. We assume that the lower metal (Region I) and the upper metal (Region III) are perfect metals, characterized by a Fermi energy E_F and a work function W. The intermediate region $0 \leqslant z \leqslant D$ is also referred to as Region II. We consider that the lower metal supports a metallic protrusion, which is part of Region II.

We assume that the junction is subject to an external bias of the form $V_{ext}(t) = V_{ext}\cos(\Omega t)$, which is actually the sum of two stimulations: $\frac{V_{ext}}{2}e^{-i\Omega t}$ and $\frac{V_{ext}}{2}e^{i\Omega t}$. The potential energy in Region II will consist of three parts. The first part $V_{stat}(\mathbf{r})$ of this potential energy contains the image potential in the vacuum [16] and the potential wells $-(E_F + W)$ used to represent the metallic elements. It is independent of the external bias. In order to determine the actual values of $V_{stat}(\mathbf{r})$, we give the material elements in Region II a dielectric constant $\epsilon = -\infty$ and we use the finite-difference techniques presented in our previous work [5, 17]. In order to determine the second part of the potential energy, which results from $\frac{V_{ext}}{2}e^{-i\Omega t}$, we give the material elements in Region II a dielectric constant $\epsilon(\Omega)$ that depends in this work on the frequency Ω (explicit expressions for tungsten and silver are provided in sections 3 and 4). The actual values of this potential energy are obtained by using the same finite-difference techniques and we express the part of the potential energy that corresponds to the stimulation $\frac{V_{ext}}{2}e^{-i\Omega t}$ as $\frac{V_{osc}(\mathbf{r},\Omega)}{2}e^{-i\Omega t}$. The third contribution to the potential energy comes from $\frac{V_{ext}}{2}e^{i\Omega t}$. It is obtained by giving the material elements in Region II a dielectric constant $\epsilon(-\Omega) = \epsilon(\Omega)^*$ and we finally express the part of the potential energy that corresponds to $\frac{V_{ext}}{2}e^{i\Omega t}$ as $\frac{V_{osc}(\mathbf{r},-\Omega)}{2}e^{i\Omega t}$. Gathering the three contributions, the potential energy in Region II that corresponds to an external bias of the form $V_{ext}(t) = V_{ext}\cos(\Omega t)$ is finally given by

$$V(\mathbf{r}, t) = V_{stat}(\mathbf{r}) + \tfrac{1}{2}[V_{osc}(\mathbf{r}, \Omega)e^{-i\Omega t} + V_{osc}(\mathbf{r}, -\Omega)e^{i\Omega t}]. \quad (1)$$

Since $V_{osc}(\mathbf{r}, -\Omega) = V_{osc}(\mathbf{r}, \Omega)^*$, $V(\mathbf{r}, t)$ is real-valued. If the dielectric constant $\epsilon(\Omega)$ is real-valued, we have furthermore $V_{osc}(\mathbf{r}, -\Omega) = V_{osc}(\mathbf{r}, \Omega) = V_{osc}(\mathbf{r})$ (a real-valued quantity that can still depend on Ω) and we return to the expression $V(\mathbf{r}, t) = V_{stat}(\mathbf{r}) + V_{osc}(\mathbf{r})\cos(\Omega t)$ used in our previous work [5, 6]. The expression (1) is however more general, as it gives the possibility for the material elements in Region II to have a potential energy $V(\mathbf{r}, t)$ that follows the oscillations of the external bias $V_{ext}(t)$ *with a phase shift* $\Delta\phi$ that depends on the position $\mathbf{r}$ and on the frequency Ω. Situations with $\Delta\phi \neq 0$ arise only when $\epsilon(\Omega)$ has an imaginary component.

One can compute the currents that flow between the two metals by using the transfer-matrix methodology presented in our previous work [18–22, 5, 6]. The idea consists in expressing the wavefunction $\Psi(\mathbf{r}, t)$ that represents the electrons provided by the two metals by

$$\Psi(\mathbf{r}, t) = \sum_{k=-N}^{N} \Psi_k(\mathbf{r})e^{-i(E+k\hbar\Omega)t/\hbar}, \quad (2)$$

where N is a cut-off parameter for the number of quanta $\hbar\Omega$ the electrons represented by $\Psi(\mathbf{r}, t)$ can absorb or emit because of their interaction with the oscillating barrier [6, 22–24]. By injecting the expressions (1) and (2) in the time-dependent Schrödinger equation $[-\frac{\hbar^2}{2m}\Delta + V(\mathbf{r}, t)]\Psi(\mathbf{r}, t) = i\hbar\frac{\partial}{\partial t}\Psi(\mathbf{r}, t)$, one obtains a system of coupled equations of the form

$$\left[-\frac{\hbar^2}{2m}\Delta + V_{stat}(\mathbf{r})\right]\Psi_k(\mathbf{r}) + \frac{1}{2}[V_{osc}(\mathbf{r}, \Omega)\Psi_{k-1}(\mathbf{r}) + V_{osc}(\mathbf{r}, -\Omega)\Psi_{k+1}(\mathbf{r})] = (E + k\hbar\Omega)\Psi_k(\mathbf{r}), \quad (3)$$

which generalizes the expression used in our previous work [6, 22]. The component $V_{osc}(\mathbf{r}, \Omega)$ of the oscillating part of the potential energy turns out to be responsible for the coupling between the components $\Psi_{k-1}(\mathbf{r})$ and $\Psi_k(\mathbf{r})$ of the wavefunction through the absorption of a quantum $\hbar\Omega$, while $V_{osc}(\mathbf{r}, -\Omega)$ is responsible for the coupling between the components $\Psi_{k+1}(\mathbf{r})$ and $\Psi_k(\mathbf{r})$ through the emission of a quantum $\hbar\Omega$.

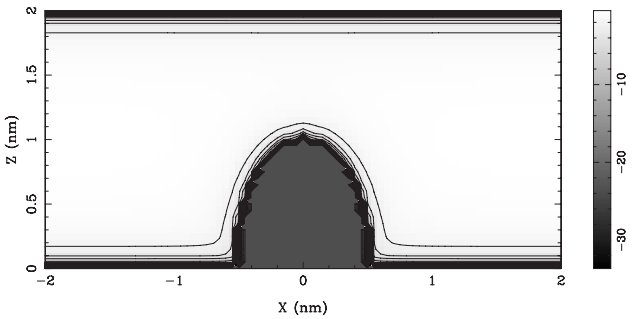

Figure 1. Static part $V_{\mathrm{stat}}(\mathbf{r})$ of the potential energy (in units of eV) in a junction made of tungsten. $V_{\mathrm{stat}}(\mathbf{r})$ includes the image potential in the vacuum and the potential wells that characterize the metallic elements.

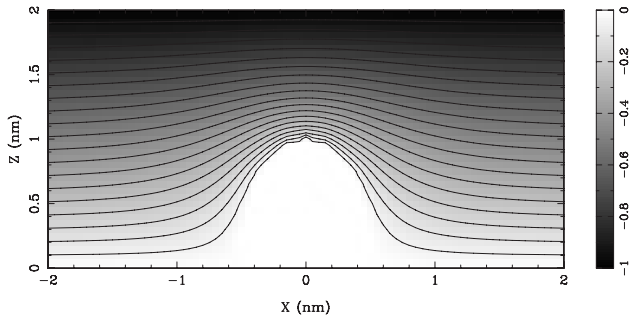

Figure 2. Oscillating part $V_{\mathrm{osc}}(\mathbf{r}, \Omega)$, in the limit when $\Omega \to 0$, of the potential energy (in units of eV) in a junction made of tungsten. $V_{\mathrm{osc}}(\mathbf{r}, \Omega)$ describes the effects of the $V_{\mathrm{ext}}(t) = V_{\mathrm{ext}} \cos(\Omega t)$ external bias, whose amplitude V_{ext} is 1 V.

The rest of the methodology is similar to that presented in our previous work [6]. We use cylindrical coordinates $\{\phi, \rho, z\}$ and assume that the electrons that cross the junction are confined in a cylinder with radius R (we take $R = 2$ nm in this work). We refer by $\Psi^{\mathrm{I},\pm}_{m,j,k}(\mathbf{r}, t)$ and $\Psi^{\mathrm{III},\pm}_{m,j,k}(\mathbf{r}, t)$ to the boundary states in Region I and III (m is the azimuthal quantum number of these states, j enumerates their radial wavevector $k_{m,j}$, and k enumerates the $2N + 1$ solutions of equation (3), which are associated with the absorption or emission of k quanta of energy $\hbar\Omega$) [6, 22]. The $\pm$ signs correspond to the propagation direction of these states relative to the z-axis. The transfer-matrix methodology provides then scattering solutions of the form

$$\Psi^{+}_{m,j,0} \overset{\mathbf{r}\in\text{Region I}}{=} \Psi^{\mathrm{I},+}_{m,j,0} + \sum_{m',j',k'} S^{-+}_{(m',j',k'),(m,j,0)} \Psi^{\mathrm{I},-}_{m',j',k'}$$
$$\overset{\mathbf{r}\in\text{Region III}}{=} \sum_{m',j',k'} S^{++}_{(m',j',k'),(m,j,0)} \Psi^{\mathrm{III},+}_{m',j',k'}, \tag{4}$$

$$\Psi^{-}_{m,j,0} \overset{\mathbf{r}\in\text{Region I}}{=} \sum_{m',j',k'} S^{--}_{(m',j',k'),(m,j,0)} \Psi^{\mathrm{I},-}_{m',j',k'}$$
$$\overset{\mathbf{r}\in\text{Region III}}{=} \Psi^{\mathrm{III},-}_{m,j,0} + \sum_{m',j',k'} S^{+-}_{(m',j',k'),(m,j,0)} \Psi^{\mathrm{III},+}_{m',j',k'}, \tag{5}$$

which correspond to single incident states $\Psi^{\mathrm{I},+}_{m,j,0}$ and $\Psi^{\mathrm{III},-}_{m,j,0}$ at the energy E, in respectively the cathode Region I and the anode Region III (the $S^{\pm\pm}_{(m',j',k'),(m,j,0)}$ provide the coefficients of the transmitted and reflected parts of these solutions) [6, 22]. Despite the use of complex-valued dielectric functions, the property $V_{\mathrm{osc}}(\mathbf{r}, -\Omega) = V_{\mathrm{osc}}(\mathbf{r}, \Omega)^*$ guarantees that the Hamiltonian $H = -\frac{\hbar^2}{2m}\Delta + V(\mathbf{r}, t)$ keeps hermitian, so that the numerical techniques presented in our previous work keep valid. These solutions enable the currents that cross the junction as well as the power gained from the source of the oscillating barrier to be calculated [6].

3. Rectification properties of a junction made of tungsten

We consider in this section that the junction is made of tungsten and we investigate the influence of the dielectric function of this material on the rectification properties of the junction. We consider as in our previous work [5, 6] that the cathode supports an hemispherical protrusion with a height of 1 nm and a radius of 0.5 nm. We also consider that the gap distance D between the two metals is 2 nm. For tungsten, we take $E_{\mathrm{F}} = 19.1$ eV as value for the Fermi energy and $W = 4.5$ eV for the work function [25].

We use for the dielectric function of tungsten a Drude's model and hence associate with the material elements in Region II a dielectric function $\epsilon(\Omega) = 1 - \Omega_{\mathrm{p}}^2/(\Omega^2 + \mathrm{i}\Omega/\tau)$ in order to describe the effects of a stimulation whose time-dependence is proportional to $\mathrm{e}^{-\mathrm{i}\Omega t}$. The plasma frequency Ω_{p} of this model was determined by $\Omega_{\mathrm{p}}^2 = \frac{ne^2}{\epsilon_0 m}$, where m is the mass of the electron, ϵ_0 is the permittivity of vacuum and $n = \frac{1}{3\pi^2}(\frac{2mE_{\mathrm{F}}}{\hbar^2})^{\frac{3}{2}}$ is the electronic density that corresponds to the Fermi energy E_{F} used for the representation of the metallic elements [25, 26]. This procedure provides a plasma energy $\hbar\Omega_{\mathrm{p}}$ of 22.8 eV, which is in fair agreement with values found in the literature [27]. We keep fully consistent with the free-electron model used to describe the cathode and the anode if we take a relaxation time $\tau = \infty$. One can however improve the representation of the material present in the junction by giving τ a value that is consistent with a property that would otherwise not be accounted for, in this case the resistivity $\rho = \frac{m}{ne^2\tau}$ of the material considered. Taking the resistivity $\rho = 5.3 \times 10^{-6}$ Ω cm of tungsten [25], we obtain a relaxation time τ of 1.8×10^{-15} s.

As explained previously, the potential energy in Region II consists of (i) a static part, which accounts for the image potential in the vacuum and for the potential wells used to represent the metallic elements, and (ii) an oscillating part, which accounts for the effects of the external bias. The static part $V_{\mathrm{stat}}(\mathbf{r})$ of the potential energy in the intermediate Region II is represented in figure 1. In the limit when $\Omega \to 0$, the dielectric function $\epsilon(\Omega)$ tends to $-\infty$, which is the value used in our previous work to describe the tip in Region II [5, 6]. The oscillating part of the potential energy $V_{\mathrm{osc}}(\mathbf{r}, \Omega)$ corresponds in this limit to the values provided in figure 2 (the amplitude V_{ext} of the external bias was given a value of 1 V). For $\hbar\Omega = 5$ eV, $\epsilon(\Omega)$ takes the value of $-19.9+1.5\mathrm{i}$. $V_{\mathrm{osc}}(\mathbf{r}, \Omega)$ is this time a complex quantity, whose real and imaginary components are represented in figure 3.

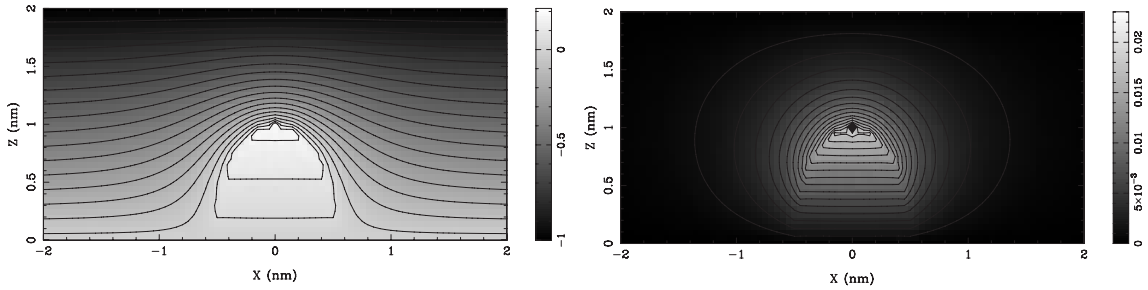

Figure 3. Real (left) and imaginary (right) components of the oscillating part $V_{\rm osc}(\mathbf{r}, \Omega)$ of the potential energy (in units of eV) in a junction made of tungsten when $\hbar\Omega = 5$ eV. $V_{\rm osc}(\mathbf{r}, \Omega)$ describes the effects of the $V_{\rm ext}(t) = V_{\rm ext}\cos(\Omega t)$ external bias, whose amplitude $V_{\rm ext}$ is 1 V.

When $\hbar\Omega$ ranges between 0 and 5 eV, $V_{\rm osc}(\mathbf{r}, \Omega)$ actually moves continuously between these two limits.

Compared to our previous work [6], in which the frequency-dependence of the dielectric function was not considered, the $V_{\rm osc}(\mathbf{r}, \Omega)$ calculated for $\hbar\Omega = 5$ eV exhibits peak values at the apex of the tip (both in the real and imaginary components). This is explained by the continuity condition for $\mathbf{D} = \epsilon_0\epsilon\mathbf{E}$. Since the dielectric constant ϵ changes from 1 in the vacuum to a negative value in the tip, the sign of the electric field $\mathbf{E}$ must change at the boundary between the tip and the vacuum. As illustrated by figure 3, the oscillating part of the potential energy has therefore a peak intensity at that boundary. This effect is more pronounced when the magnitude of $\epsilon(\Omega)$ is small, which is the case for large values of $\hbar\Omega$. In the limit when $\Omega \to 0$, $\epsilon(\Omega) \to -\infty$ and the continuity condition for $\mathbf{D}$ rather predicts an electric field $\mathbf{E} = 0$ at the apex of the tip so that these peak values in the oscillating part of the potential energy do not appear. We return in this limit to the values provided in figure 2.

In order to determine the impact of the frequency-dependence of $\epsilon(\Omega)$ on the properties of the junction, we represented in figure 4 the mean value $\langle P\rangle$ of the power gained by the electrons that cross the junction from the source of the external bias. This figure actually compares the results achieved by using $\epsilon(\Omega) = -\infty$, $\epsilon(\Omega) = 1 - \Omega_{\rm p}^2/\Omega^2$ and $\epsilon(\Omega) = 1 - \Omega_{\rm p}^2/(\Omega^2 + {\rm i}\Omega/\tau)$ as model for the dielectric function of the tip. The results correspond to an amplitude $V_{\rm ext}$ of the external bias of respectively 1, 0.1 and 0.01 V. The results show that the frequency-dependence of the dielectric function is actually responsible for the predicted values of $\langle P\rangle$ to be larger than in the case where we simply assume that $\epsilon(\Omega) = -\infty$. For $\hbar\Omega = 2.5$ eV, the difference is of the order of 7%. This difference increases with $\hbar\Omega$ and is of the order of 40% for $\hbar\Omega = 5$ eV. The relaxation time τ on the other hand turns out to have a smaller impact on these results. Compared to the values obtained using $\epsilon(\Omega) = 1 - \Omega_{\rm p}^2/\Omega^2$ as model for the dielectric function, $\langle P\rangle$ is increased by typically 1% when the imaginary part of $\epsilon(\Omega)$ is considered. This is reflected by the fact the imaginary part of $V_{\rm osc}(\mathbf{r}, \Omega)$ is at least two orders of magnitude smaller than the real part of $V_{\rm osc}(\mathbf{r}, \Omega)$ when we consider $\hbar\Omega$ values between 0 and 5 eV. This increase in the power gained by the electrons that cross the junction is consistent with the fact the imaginary part of $\epsilon(\Omega)$ usually describes an absorption of the electromagnetic radiations.

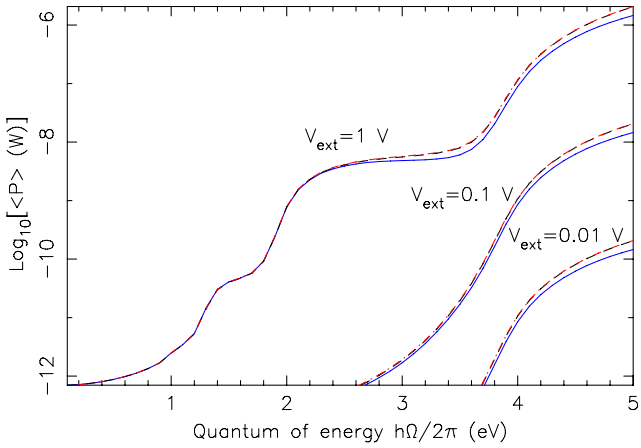

Figure 4. Power gained by the electrons that cross the junction from the source of the oscillating barrier. The junction is made of tungsten and subject to an external bias $V_{\rm ext}(t) = V_{\rm ext}\cos(\Omega t)$, with $V_{\rm ext} = 1$, 0.1 and 0.01 V (downwards, as indicated). The solid, dashed and dot–dashed lines indicate results achieved respectively with $\epsilon(\Omega) = -\infty$, $\epsilon(\Omega) = 1 - \Omega_{\rm p}^2/\Omega^2$ and $\epsilon(\Omega) = 1 - \Omega_{\rm p}^2/(\Omega^2 + {\rm i}\Omega/\tau)$ as model for the dielectric function of the tip.

Besides the mean power $\langle P\rangle$ gained by the electrons that cross the junction, another quantity of interest for the development of technologies is the rectification ratio $R = \langle I^+\rangle/\langle I^-\rangle$ one obtains by taking the ratio between the mean value of the upward current ($\langle I^+\rangle$) and the mean value of the downward current ($\langle I^-\rangle$). This quantity indicates indeed the ability of the junction to provide a current with a strong dc component when subject to an alternating voltage. We represented in figure 5 the rectification ratio that characterizes the tungsten junction. We compare as previously the results achieved with the three models of the dielectric function and an amplitude $V_{\rm ext}$ of the external bias of 1, 0.1 and 0.01 V. The differences with the results achieved using $\epsilon(\Omega) = -\infty$ as model for the dielectric function of the tip become significant starting from $\hbar\Omega = 2.2$ eV. Because of its impact on the oscillating part of the potential energy (especially at the apex of the tip), the frequency-dependence of the dielectric function tends to increase the mean value of the upward current $\langle I^+\rangle$, which enhances the rectification ratio R. We observe as in our previous work a decrease of the rectification ratio for $\hbar\Omega$ values around 4 eV (it was estimated that the bias then reverses before the electrons can cross the junction) [6].

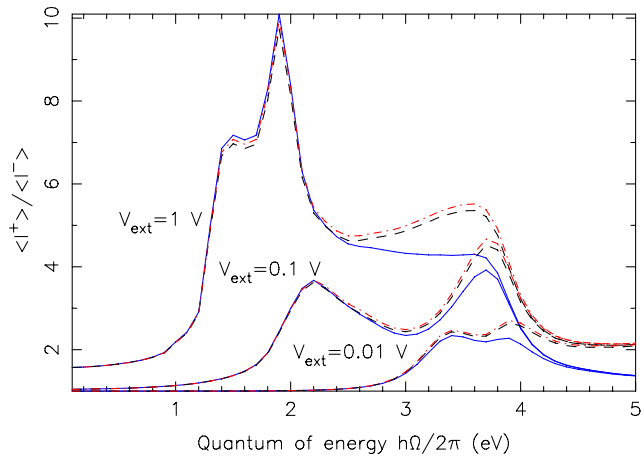

Figure 5. Rectification ratio of a junction made of tungsten and subject to an external bias $V_{\rm ext}(t) = V_{\rm ext}\cos(\Omega t)$, with $V_{\rm ext} = 1$, 0.1 and 0.01 V (downwards as indicated). The solid, dashed and dot–dashed lines indicate results achieved respectively with $\epsilon(\Omega) = -\infty$, $\epsilon(\Omega) = 1 - \Omega_{\rm p}^2/\Omega^2$ and $\epsilon(\Omega) = 1 - \Omega_{\rm p}^2/(\Omega^2 + {\rm i}\Omega/\tau)$ as model for the dielectric function of the tip.

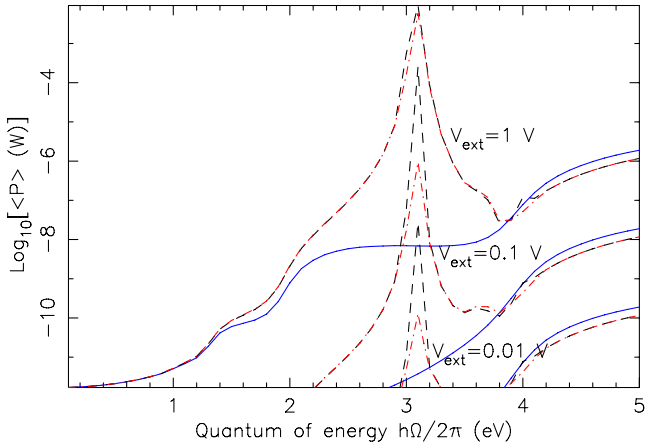

Figure 6. Power gained by the electrons that cross the junction from the source of the oscillating barrier. The junction is made of silver and subject to an external bias $V_{\rm ext}(t) = V_{\rm ext}\cos(\Omega t)$, with $V_{\rm ext} = 1$, 0.1 and 0.01 V (downwards, as indicated). The solid, dashed and dot–dashed lines indicate results achieved respectively with $\epsilon(\Omega) = -\infty$, $\epsilon(\Omega) = \epsilon_\infty - \Omega_{\rm p}^2/\Omega^2$ and $\epsilon(\Omega) = \epsilon_\infty - \Omega_{\rm p}^2/(\Omega^2 + {\rm i}\Gamma\Omega)$ as model for the dielectric function of the tip.

4. Rectification properties of a junction made of silver

The plasma energy $\hbar\Omega_{\rm p}$ of tungsten was given a value of 22.8 eV, which is much larger than the values considered for the quantum of energy $\hbar\Omega$ the electrons that cross the junction can absorb or emit because of their interaction with the oscillating barrier (we only consider values between 0 and 5 eV). This explains why the rectification properties of the junction exhibit a limited sensitivity on the frequency-dependence of the dielectric function when tungsten is used as material for the tip. Silver has a surface plasmon energy of 3.6 eV and a bulk plasmon energy of 3.78 eV [15]. This experimental value for the surface plasmon of silver corresponds to a situation in which silver is delimited by a flat surface. The situation considered in this paper is however different because of the presence of the tip. This tip exhibits indeed a plasmon at an energy that is smaller than in the case of a flat surface. The energy of this plasmon is still in the range of values considered for $\hbar\Omega$ and it is therefore interesting to investigate the effects that arise when silver is used as material for the tip instead of tungsten. We will first consider the consequences on the mean power $\langle P\rangle$ and on the rectification ratio R that characterize the junction. We will then relate the variations of these quantities to the potential energy in the junction.

In order to simulate a junction made of silver, we take a Fermi energy $E_{\rm F}$ of 5.48 eV and a work function W of 4.52 eV [25]. We refer to the expression $\epsilon(\Omega) = \epsilon_\infty - \Omega_{\rm p}^2/(\Omega^2 + {\rm i}\Gamma\Omega)$ given by Kawata *et al* for the dielectric function of silver, in which $\epsilon_\infty = 4.9638$, $\Omega_{\rm p} = 1.4497 \times 10^{16}$ s^{-1} and $\Gamma = 8.33689 \times 10^{13}$ s^{-1} (these coefficients were adjusted on experimental data that cover the visible spectrum) [28]. As for tungsten, we will actually present results achieved using $\epsilon(\Omega) = -\infty$, $\epsilon(\Omega) = \epsilon_\infty - \Omega_{\rm p}^2/\Omega^2$ and $\epsilon(\Omega) = \epsilon_\infty - \Omega_{\rm p}^2/(\Omega^2 + {\rm i}\Gamma\Omega)$ as model for the dielectric function of the tip.

The mean value $\langle P\rangle$ of the power gained by the electrons that cross the junction, when silver is used as material for the tip, is represented in figure 6. The figure includes as previously results obtained for an amplitude $V_{\rm ext}$ of the external bias of 1, 0.1 and 0.01 V. The consideration of silver as material for the tip makes a significant difference compared to tungsten, especially for $\hbar\Omega$ values in the interval between 2 and 4 eV. As for tungsten, the reduction in the magnitude of the dielectric function of the tip, in a range of frequencies for which its real part is still negative, results in an enhancement of $\langle P\rangle$. The maximal value is achieved for $\hbar\Omega$ around 3.1 eV, which is the energy at which the tip has a resonant polarization (this value is in agreement with the typical energies observed for small clusters) [29]. Compared to the values of $\langle P\rangle$ obtained with tungsten, there is an enhancement by six orders of magnitude around that energy. This spectacular enhancement arises in conditions where the energy $\hbar\Omega$ at which the polarization resonance occurs is comparable with the height of the surface barrier. We note that the power $\langle P\rangle$ predicted for $V_{\rm ext} = 1$ V in the case of a junction made of silver may be to large to be sustained by a realistic device, so that values of 0.1 V at most shall be used in applications. We note finally that $\epsilon(\Omega) = \epsilon_\infty - \Omega_{\rm p}^2/\Omega^2$ represents a good approximation for the dielectric function of the tip as long as $\hbar\Omega$ does not correspond to the energy at which the system goes through a resonance. When this situation occurs, it is essential to use a model for $\epsilon(\Omega)$ that includes dissipation.

The replacement of tungsten by silver has also a significant impact on the rectification ratio of the junction. This is illustrated by figure 7, where we represented the results achieved with an amplitude $V_{\rm ext}$ for the external bias of 1, 0.1 and 0.01 V. The results show that a rectification ratio as high as 0.8×10^5 is achieved for $\hbar\Omega = 3.2$ eV and $V_{\rm ext} = 1$ V (the mean upward current takes in this case a value of 1.1×10^{-5} A). As for the power gained by the electrons that cross the junction,

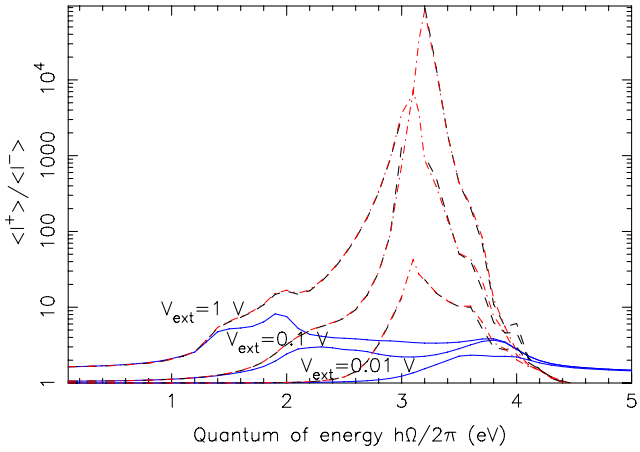

Figure 7. Rectification ratio of a junction made of silver and subject to an external bias $V_{\rm ext}(t) = V_{\rm ext}\cos(\Omega t)$, with $V_{\rm ext} = 1$, 0.1 and 0.01 V (downwards, as indicated). The solid, dashed and dot–dashed lines indicate results achieved respectively with $\epsilon(\Omega) = -\infty$, $\epsilon(\Omega) = \epsilon_\infty - \Omega_{\rm p}^2/\Omega^2$ and $\epsilon(\Omega) = \epsilon_\infty - \Omega_{\rm p}^2/(\Omega^2 + {\rm i}\Gamma\Omega)$ as model for the dielectric function of the tip. Results obtained at the 3.1 eV resonance energy with $\epsilon(\Omega) = \epsilon_\infty - \Omega_{\rm p}^2/\Omega^2$ as model for the dielectric function of the tip were not represented.

the frequency-dependence of the dielectric function plays a significant role. For comparison, a rectification ratio of 9.95 only is achieved with $V_{\rm ext} = 1$ V when tungsten is used as material for the tip. As for tungsten, we observe a significant decrease of the rectification ratio for $\hbar\Omega$ values around 4 eV in agreement with our previous analysis [6].

In order to illustrate how these results are actually affected by the occurrence of a surface plasmon for $\hbar\Omega = 3.1$ eV and, more generally, in order to relate these results to the variations of the dielectric function of the tip, we finally represented in figure 8 the real part of $V_{\rm osc}(\mathbf{r}, \Omega)$ at four representative values of $\hbar\Omega$: 3, 3.2, 3.8 and 5 eV (we took 1 V for the amplitude $V_{\rm ext}$ of the external bias). For $\hbar\Omega = 3$ eV, which is just below the polarization resonance, we have $\epsilon(\Omega) = -5.15 + 0.18$i. As for tungsten, the fact the real part of $\epsilon(\Omega)$ changes sign when going from the tip into the vacuum is responsible for the oscillating part of the potential energy to have a maximal intensity at the apex of the tip. This enhances the absorption of quanta by the electrons in the tip and increases the emission. As we continue increasing the frequency, the dielectric function of the tip and of the medium become comparable in magnitude. The surface of the tip has progressively a stronger influence on its polarization. A polarization resonance is finally reached for $\hbar\Omega$ around 3.1 eV and the oscillating part of the potential energy suddenly goes from a large positive value at the apex of the tip to a large negative value. This is well illustrated for $\hbar\Omega = 3.2$ eV, where $\epsilon(\Omega) = -3.93 + 0.15$i. The oscillating part of the potential energy is now smaller in magnitude, which reduces the emission. The depression that characterizes the real part of $V_{\rm osc}(\mathbf{r}, \Omega)$ at the apex of the tip vanishes progressively as we continue increasing the frequency. For $\hbar\Omega = 3.8$ eV, we have $\epsilon(\Omega) = -1.34 + 0.09$i and the depression in the values of $V_{\rm osc}(\mathbf{r}, \Omega)$ has essentially disappeared. The fact the real part of $\epsilon(\Omega)$ is negative results in the equipotentials of $V_{\rm osc}(\mathbf{r}, \Omega)$ to be deflected towards the tip. This picture still changes when the real part of $\epsilon(\Omega)$ becomes positive. For ${\rm Re}[\epsilon(\Omega)] > 1$, these equipotentials rather tend to bypass the tip. For $\hbar\Omega = 5.0$ eV, we have $\epsilon(\Omega) = 1.32 + 0.04$i. The contrast between the dielectric constant of the tip and that of the medium is relatively small at this point, so that the tip is essentially transparent to the field.

The results achieved with silver differ from those achieved with tungsten essentially by the fact a polarization resonance is encountered in the range of frequencies considered. For frequencies Ω that are above this resonance, the dielectric function $\epsilon(\Omega)$ is small in magnitude so that the tip becomes essentially transparent to the field. This reduces the emission of current from the tip, compared to the values achieved with

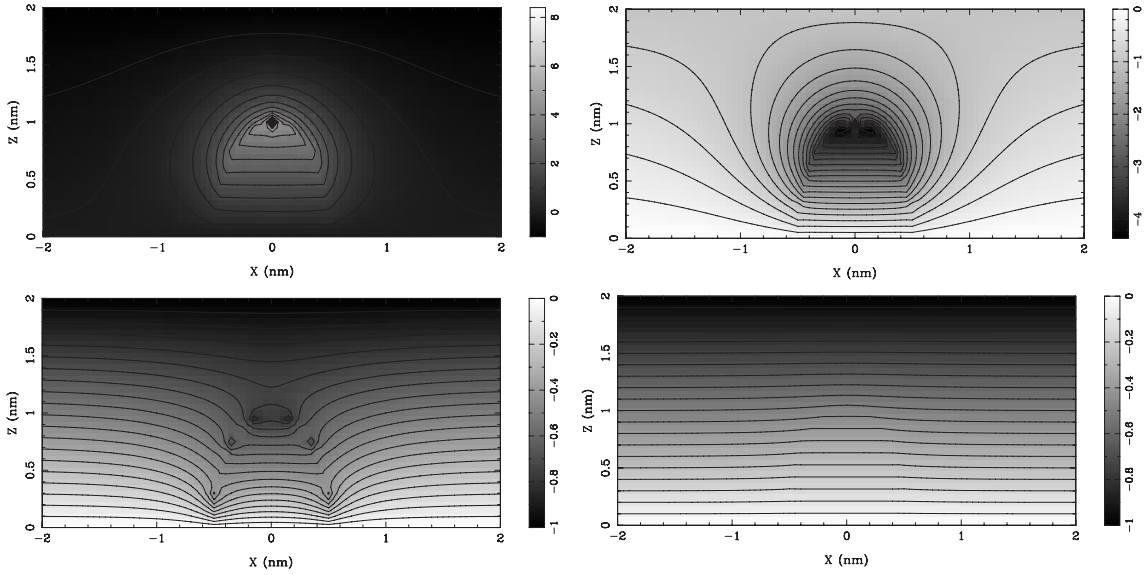

Figure 8. Real component of the oscillating part $V_{\rm osc}(\mathbf{r}, \Omega)$ of the potential energy (in units of eV) in a junction made of silver. $V_{\rm osc}(\mathbf{r}, \Omega)$ describes the effects of the $V_{\rm ext}(t) = V_{\rm ext}\cos(\Omega t)$ external bias, whose amplitude $V_{\rm ext}$ is 1 V. The representation corresponds to $\hbar\Omega = 3$ eV (top left), 3.2 eV (top right), 3.8 eV (bottom left) and 5 eV (bottom right).

a model where $\epsilon(\Omega) = -\infty$, in which the tip follows the stimulation of the external field. The mean values of the power $\langle P \rangle$ and of the rectification ratio R, which are essentially proportional to the mean value of the upward current $\langle I^+ \rangle$, are therefore *smaller* than the values achieved for $\epsilon(\Omega) = -\infty$ at these frequencies. In the case of tungsten, the frequencies Ω considered are below the polarization resonance. As explained previously, the frequency-dependence of the dielectric function $\epsilon(\Omega)$ rather enhances the emission of current from the tip, which results in *larger* values of $\langle P \rangle$ and R compared to the values achieved with a model where $\epsilon(\Omega) = -\infty$. This explains the differences observed in the limit of high frequencies between tungsten and silver.

The results achieved for $\langle P \rangle$ in the case of tungsten or silver are not merely proportional to V_{ext}^2, because of the occurrence of multi-photon absorption processes in the junction (this is especially the case when $\hbar\Omega \ll |eV_{\text{ext}}|$) [6]. These non-linearities in the dependence of $\langle P \rangle$ with respect to V_{ext}^2 actually lead to an enhancement of the values of $\langle P \rangle$. This effect is more pronounced when a polarization resonance occurs, which is the case for silver. This explains both the magnification and the broadening of the resonance observed with silver as the amplitude V_{ext} of the external bias increases.

The transition between the range of frequencies at which an enhancement of the emission is obtained and the range of frequencies at which the tip is essentially transparent to the field will in general depend on a variety of factors, which include the material, the shape and the size of the tip. These factors determine indeed the energy at which surface plasmons will arise. Since these plasmons determine in turn the position of this transition, our results actually suggest that the frequency at which the junction is the most efficient for the rectification of external signals or for the conversion of their energy could be controlled by these parameters.

5. Conclusion

We used a transfer-matrix methodology to study the rectification properties of geometrically asymmetric metal–vacuum–metal junctions in which one of the metals is essentially flat while the other is extended by a tip. We considered in particular the role of the dielectric function of the tip on the power gained by the electrons that cross the junction. We also calculated the rectification ratio of this device, which characterizes its ability to rectify ac voltages. We compared for this study junctions made of either tungsten or silver. For the geometry considered in this paper, the rectification ratio of the device as well as the power it could provide to an external load were enhanced by several orders of magnitude for $\hbar\Omega$ values around 3.1 eV when silver was used as material for the tip. This enhancement in the rectification properties of the junction was related to a resonant polarization of the tip. It appears therefore that this process could used to control the frequency at which the device is the most efficient for the rectification of external signals (this control could be achieved through the geometry or the material used for the tip). This opens the possibility to build devices of the type presented in this paper for the selective detection of radiations in the infrared or optical domain or for a more efficient conversion of their energy.

Acknowledgments

This work was funded by the National Fund for Scientific Research (FNRS) of Belgium. The authors acknowledge the use of the Inter-university Scientific Computing Facility (ISCF) of Namur. C Vandenbem is acknowledged for valuable suggestions. J-P Vigneron and A A Lucas are acknowledged for their interest in this problem.

References

[1] Sullivan T E, Cutler P H and Lucas A A 1976 *Surf. Sci.* **54** 561
[2] Lucas A A, Moussiaux A, Schmeits M and Cutler P H 1977 *Commun. Phys.* **2** 169
[3] Miskovsky N M, Shepherd S J, Cutler P H, Sullivan T E and Lucas A A 1979 *Appl. Phys. Lett.* **35** 560
[4] Sullivan T E, Kuk Y and Cutler P H 1989 *IEEE Trans. Electron Devices* **36** 2659
[5] Mayer A, Chung M S, Weiss B L, Miskovsky N M and Cutler P H 2008 *Phys. Rev.* B **77** 085411
[6] Mayer A, Chung M S, Weiss B L, Miskovsky N M and Cutler P H 2008 *Phys. Rev.* B **78** 205404
[7] Evenson K H, Day G W, Wells J S and Mullen L O 1972 *Appl. Phys. Lett.* **20** 133
[8] Krieger W, Suzuki T, Volcker M and Walther H 1980 *Phys. Rev.* B **41** 10229
[9] Miskovsky N M, Park S H, Cutler P H and Sullivan T E 1994 *J. Vac. Sci. Technol.* B **12** 2148
[10] Fumeaux C, Herrmann W, Kneubuhl F K and Rothuizen H 1998 *Infrared Phys. Technol.* **39** 123
[11] Beverini N, Carelli G, Ciaramella E, Contestabile G, DeMichele A and Presi M 2005 *Laser Phys.* **15** 1334
[12] Bava E, Beverini N, Carelli G, De Michele A, Galzerano G, Maccioni E, Moretti A, Prevedelli M, Sorrentino F and Svelto C 2005 *IEEE Trans. Instrum. Meas.* **54** 1407
[13] Nguyen H Q, Cutler P H, Feuchtwang T E, Huang Z-H, Kuk Y, Silverman P J, Lucas A A and Sullivan T E 1989 *IEEE Trans. Electron Devices* **36** 2671
[14] Hartman T E 1962 *J. Appl. Phys.* **33** 3427
[15] Daniels J, Festenburg C, Raether H and Zeppenfield K 1970 *Tracts in Modern Physics* vol 54 (Berlin: Springer) p 77
[16] Laloyaux Th, Derycke I, Vigneron J-P, Lambin Ph and Lucas A A 1993 *Phys. Rev.* B **47** 7508
[17] Mayer A and Lambin Ph 2005 *Nanotechnology* **16** 2685
[18] Mayer A and Vigneron J-P 1999 *Ultramicroscopy* **79** 35
[19] Mayer A and Vigneron J-P 1999 *J. Vac. Sci. Technol.* B **17** 506
[20] Mayer A and Vigneron J-P 1999 *Phys. Rev.* E **60** 7533
[21] Mayer A and Vigneron J-P 2000 *Phys. Rev.* E **61** 5953
[22] Mayer A and Vigneron J-P 2000 *Phys. Rev.* B **62** 16138
[23] Faisal F H M 1987 *Theory of Multiphoton Processes* (New York: Plenum) pp 8–10
[24] Pimpale A, Holloday S and Smith R J 1991 *J. Phys. A: Math. Gen.* **24** 3533
[25] Kittel C 1998 *Physique de l'Etat Solide* 7th edn (Paris: Dunod) p 132, 146 and 499
[26] Lenham A P and Treherne D M 1969 *Optical Properties and Electronic Structure of Metals and Alloys* ed F Abeles (Amsterdam: North-Holland) p 199
[27] Luscher P E 1977 *Surf. Sci.* **66** 167
[28] Kawata S, Ono A and Verma P 2008 *Nat. Photon.* **2** 438
[29] Mayer A, Gonzalez A, Aikens C M and Schatz G C 2009 *Nanotechnology* **20** 195204